**HEFAT2014**
**10th International Conference on Heat Transfer, Fluid Mechanics and Thermodynamics**
**14 – 16 July 2014**
**Orlando, Florida**

# SPREADING RESISTANCE IN ANISOTROPIC RECTANGULAR PLATES WITH MULTIPLE HEAT SOURCES AND SINKS

Gholami A. and Bahrami M.*
*Author for correspondence
Laboratory for Alternative Energy Conversion (LAEC)
School of Mechatronic Systems Engineering
Simon Fraser University, Surrey, BC, Canada, V3T 0A3
E-mail: mbahrami@sfu.ca

## ABSTRACT

In this study, a new analytical model for temperature distribution inside anisotropic rectangular plates subjected to multiple cold/hotspots on the top and bottom surfaces is presented. All lateral faces are assumed to be insulated. 2-D Fourier expansion technique is used to transform the discrete Neumann boundary conditions on the top and bottom into a continuous form. The solution is first justified for the case with single hotspots on each side and then using the superposition principle, it is extended into the general form to cover multi-hotspot cases. The model is validated by numerical simulation data and a perfect agreement is observed. Thermal spreading resistance is defined for the anisotropic plate and a parametric study for optimization purpose is performed. The influence of anisotropy on the resistance is discussed in detail and critical values are evaluated.

## INTRODUCTION

Recently, graphite-based anisotropic materials have received a significant attention due to their exceptional thermo-physical properties [1–3]. Graphite-based materials are one of the well-known anisotropic materials which have in-plane thermal conductivities, up to 1500 W/m.K, and through-plane thermal conductivities around 2 W/m.K.[3–6]. This property is mainly due to their especial atomic structure. They are generally, a stack of Graphene flakes piled upon each other (Fig. 1). The interlayer cohesive energy of Graphene flakes which is due to the van der Waals atomic attraction is much stronger than intralayer covalent bonding [7]. This structural feature causes large anisotropy in graphite which makes it an ideal candidate for heat spreaders where higher heat transfer is desired in in-plane than in the through-plane direction. Heat spreaders are one of the main components in any cooling systems of electronic, power electronic, photonics, and telecom devices. They reduce heat flux at hotspots by spreading it into larger area. [8], [9]. The spreading (or constriction) resistance causes an extra resistance against the heat flow which can be minimized by properly designing the spreader.

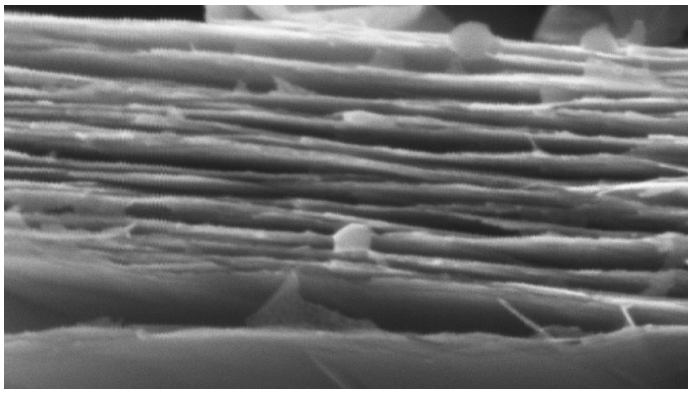

**Figure 1.** SEM image of compressed expanded graphite

A number of relevant analytical and numerical studies can be found on this topic in the literature. Most of the existing works were focused only on isotropic materials. Kokkas [10] obtained a general quasi-equilibrium Fourier/Laplace transform solution for a rectangular slab with heat sources on top and convective cooling on the bottom. Kadambi and Abuaf [11] developed an analytical solution to axisymmetric as well as 3-D steady-state and transient heat conduction equations for a convectively cooled slab with a heat source at the center of the top surface. Yovanovich *et al.* [8] reported a general expression for spreading resistance of a heat source centered on a rectangular double layer plate with either conduction or convection on the bottom surface. They also presented closed-form spreading resistance relationships for several special cases. Culham *et al.* [12] reported a more general solution to the 3-D Laplace equation for the rectangular plate with centered heat source on the top and edge cooling instead of insulation on the side walls. Later, Muzychka *et al.* [13] extended Culham *et al.* work and solved the same problem in cylindrical coordinates for a circular slab. In another study, they [14] reported a general solution for thermal spreading resistances of convectively cooled rectangular flux channel with eccentric heat sources on top. Using a superposition technique,

Muzychka [15] generalized the solution for problems with multi-heat sources on the top. He introduced the "influence coefficient", which defines the contribution of each heat source on the temperature rise of other hotspots. Employing an asymptotic approach, Karmalkar *et al.* [9] proposed a closed-form expression for spreading resistance for all rectangular and circular hotspot contact conditions. Recently, Dan *et al.* [16] presented a solution to temperature distribution inside a multi-layered isotropic rectangular tube with discrete isothermal hotspots on both top and bottom surfaces. To overcome the complexity of the mixed boundary conditions they employed an approximate technique to convert this boundary condition into a Neumann boundary condition.

There are only a few analytic studies on 3-D conduction heat transfer in anisotropic materials subjected to discrete heat flux in the literature. Ying and Toh [17] developed an anisotropic spreading resistance model in cylindrical coordinates for a disc with centric heat source on the top and convective cooling on the bottom. Muzychka *et al.* [18] brought a summary of all the previous studies for isotropic materials and by transforming the boundary conditions and governing equations for anisotropic systems, obtained a new solution for convectively cooled rectangular flux channels as well as circular flux tubes with centralized heat source on the top.

In the present study, a new general solution to 3-D conduction heat transfer in anisotropic rectangular plate ($k_x \neq k_y \neq k_z$) with multiple heat sources and heat sinks on the top and bottom surfaces is presented. The present model is validated by an independent numerical study. It is found that in electronic devices where heat is required to travel in-plane from the hotspot to get to the sink, which is the case of notebooks and cell phones, properly designed anisotropic spreaders perform much better than conventional isotropic metallic ones.

## NOMENCLATURE

| | | |
|---|---|---|
| *A,B,C* | [-] | Solution coefficients |
| *H* | [m] | Plate thickness |
| *L* | [m] | Plate length |
| *M* | [-] | Number of sources/sinks on the top surface |
| *N* | [-] | Number of sources/sinks on the bottom surface |
| *Q* | [W] | Total heat flow |
| $Q_{ref}$ | [W] | Reference heat flow |
| *T* | [K] | Temperature |
| $T_0$ | [K] | Reference temperature |
| *W* | [m] | Plate width |
| *X* | [m] | *x* coordinate of source/sink's center |
| *Y* | [m] | *y* coordinate of source/sink's center |
| *a* | [m] | Length of source/sink |
| *b* | [m] | Width of source/sink |
| *s* | [-] | Fourier series coefficient |
| *k* | [W/mK] | Thermal conductivity |
| *m,n* | [-] | Term number in series solution |
| *q* | [W/m$^2$] | Heat flux |

Special characters

| | | |
|---|---|---|
| *β, δ, λ* | [-] | Eigenvalue (*x-y-z* direction) |
| *ε* | [-] | Width to length aspect ratio of the plate |
| $\varepsilon_H$ | [-] | Height to length aspect ratio of the plate |
| *κ* | [-] | Dimensionless thermal conductivity |

Subscripts

| | |
|---|---|
| *i* | Number of sources/sinks on each surface |
| *source* | Pertaining to heat sources |
| *sink* | Pertaining to heat sinks |

Superscripts

| | |
|---|---|
| * | Specifies dimensionless parameter |
| *t* | Top surface |
| *b* | Bottom surface |

## MODEL DEVELOPMENT

An anisotropic rectangular plate of L×W with thickness of H (Fig. 2.a) is considered for the following two scenarios:

i) Subjected to a single rectangular source and sink arbitrary-located on the both top and bottom surface and,

ii) More generally, subjected to 'M' and 'N' arbitrarily located sinks and sources on the top and bottom surface.

As boundary conditions, it is assumed that the lateral faces of the plate are insulated, i.e., no heat transfer through the side walls. All the top and bottom surfaces except at the spots (refers to either hot or cold-spots) are also considered to be insulated. Spots have arbitrary heat flux, (i is the number assigned to spots), positive values for heat sources and negative for sinks, which are functions of x and y. Each spot is centrally positioned at x coordinate of X and y coordinate of Y with length and width of a and b, respectively, as shown in Fig. 2.b. The objectives are to: i) find the temperature distribution inside the plate with any arbitrarily arrangement of spots on the top and bottom surfaces analytically, and ii) define corresponding spreading resistance.

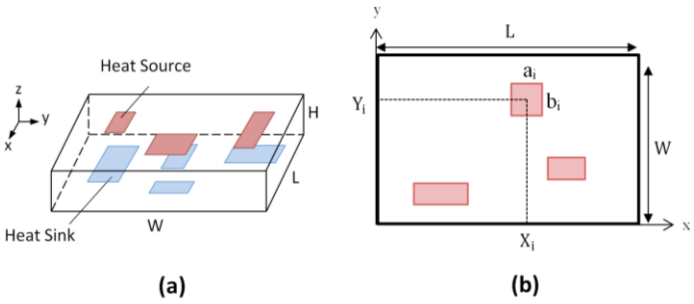


**Figure 2** Schematic of an anisotropic rectangular spreader with multiple hotspots on the top and bottom surfaces (a) Size and location of the hotspots (b)

### General solution

Dimensionless parameters are defined as follows and the governing equation and boundary conditions are expressed accordingly.

$$\varepsilon = \frac{W}{L}, \quad \varepsilon_H = \frac{H}{L}, \quad x^* = \frac{x}{L}, \quad y^* = \frac{y}{L}, \quad z^* = \frac{z}{L}$$

$$a_i^* = \frac{a_i}{L}, \quad b_i^* = \frac{b_i}{L}, \quad q_{i(x,y)}^* = \frac{L^2 q_{i(x,y)}}{Q_{ref}}, \quad \theta = \frac{Lk_z}{Q_{ref}}(T - T_0)$$

$$\kappa_x = \sqrt{\frac{k_z}{k_x}}, \quad \kappa_y = \sqrt{\frac{k_z}{k_y}}, \quad R^* = Lk_z R \qquad (1)$$

where is an arbitrary reference heat flux and is a reference temperature. Using the parameters in Eq. (1), the dimensionless form of the governing equation and the boundary conditions are:

$$\nabla^2\theta = \frac{1}{\kappa_x^{\,2}}\frac{\partial^2\theta}{\partial x^{*2}} + \frac{1}{\kappa_y^{\,2}}\frac{\partial^2\theta}{\partial y^{*2}} + \frac{\partial^2\theta}{\partial z^{*2}} = 0 \tag{2}$$

$$\begin{aligned} &\frac{\partial\theta}{\partial x^*} = 0 && at\ \ x^* = 0,\ x^* = 1 \\ &\frac{\partial\theta}{\partial y^*} = 0 && at\ \ y^* = 0,\ y^* = \varepsilon \end{aligned} \tag{3}$$

$$\text{at } z^* = 0 \rightarrow \begin{cases} \dfrac{\partial\theta}{\partial z^*} = q_{i(x,y)}^{\,*} & \text{at spot 'i' domain} \\ \dfrac{\partial\theta}{\partial z^*} = 0 & \text{at remainder} \end{cases} \tag{4}$$

$$\text{at } z^* = \varepsilon_H \rightarrow \begin{cases} \dfrac{\partial\theta}{\partial z^*} = q_{i(x,y)}^{'\,*} & \text{at spot 'i' domain} \\ \dfrac{\partial\theta}{\partial z^*} = 0 & \text{at remainder} \end{cases}$$

Using a separation of variable technique, Eq. (2) has the general solution in the form of below:

$$\theta = \sum_{\lambda}\sum_{\delta} C_{(\lambda,\delta)}\, e^{\lambda\kappa_x x^*} e^{\delta\kappa_y y^*} e^{i\sqrt{\lambda^2+\delta^2}\,z^*} \tag{5}$$

In witch, $\lambda$, $\delta$ and $C_{(\lambda,\delta)}$ are unknown coefficients that should be defined through applying the boundary conditions. Applying the first boundary conditions, Eq. (3), and expanding the solution into trigonometric form results:

$$\begin{aligned} \theta &= A_0 z^* \\ &+ \sum_{m=1}^{\infty} \cos\left(\lambda\kappa_x x^*\right) \times \left[ A_m \cosh\left(\lambda z^*\right) + B_m \sinh\left(\lambda z^*\right) \right] \\ &+ \sum_{n=1}^{\infty} \cos\left(\delta\kappa_y y^*\right) \times \left[ A_n \cosh\left(\delta z^*\right) + B_n \sinh\left(\delta z^*\right) \right] \\ &+ \sum_{n=1}^{\infty}\sum_{m=1}^{\infty} \cos\left(\lambda\kappa_x x^*\right)\cos\left(\delta\kappa_y y^*\right) \times \left[ A_{mn} \cosh\left(\beta z^*\right) + B_{mn} \sinh\left(\beta z^*\right) \right] \end{aligned} \tag{6}$$

where $\lambda$, $\delta$ and $\beta$ are eigenvalues in the form of below:

$$\lambda = \frac{m\pi}{\kappa_x}, \qquad \delta = \frac{n\pi}{\kappa_y \varepsilon}, \qquad \beta = \sqrt{\lambda^2+\delta^2} \tag{7}$$

In the Eq. (6) '*A*'s, '*B*'s are coefficients which should be defined by applying the boundary conditions on the top and bottom surfaces. As it is shown in Eq. (4), the Neumann boundary conditions on these two surfaces have a discrete form which cannot directly be applied. To apply these boundary conditions in the solution, Eq. (6), a 2-D Fourier expansion technique is used. Using this technique, the temperature distribution is derived for single and multi-hotspots cases.

*i) Single heat source and heat sink*

For a plate with one heat source on the top surface (subscript t) and one heat sink on the bottom (subscript b), the coefficients of the solution, Eq. (9), are as follows:

$$A_0 = \frac{s_{00}^t}{\varepsilon} = \frac{s_{00}^b}{\varepsilon} \tag{8}$$

$$B_m = \frac{2s_{m0}^t}{\varepsilon\lambda} \tag{9}$$

$$B_n = \frac{2s_{0n}^t}{\varepsilon\delta} \tag{10}$$

$$B_{mn} = \frac{4s_{mn}^t}{\varepsilon\beta} \tag{11}$$

$$A_m = \frac{2}{\varepsilon\lambda}\left( s_{m0}^b \operatorname{csch}\left(\lambda\varepsilon_H\right) - s_{m0}^t \coth\left(\lambda\varepsilon_H\right) \right) \tag{12}$$

$$A_n = \frac{2}{\varepsilon\delta}\left( s_{0n}^b \operatorname{csch}\left(\delta\varepsilon_H\right) - s_{0n}^t \coth\left(\delta\varepsilon_H\right) \right) \tag{13}$$

$$A_{mn} = \frac{4}{\varepsilon\beta}\left( s_{mn}^b \operatorname{csch}\left(\beta\varepsilon_H\right) - s_{mn}^t \coth\left(\beta\varepsilon_H\right) \right) \tag{14}$$

In which the auxiliary coefficients, obtained from Furrier expansion, are:

$$s_{00}^{t\ or\ b} = \iint_{t\ or\ b} q_{(x,y)}^*\, dx^* dy^* \tag{15}$$

$$s_{m0}^{t\ or\ b} = \iint_{t\ or\ b} q_{(x,y)}^* \times \cos\left(\lambda\kappa_x x^*\right) dx^* dy^* \tag{16}$$

$$s_{0n}^{t\ or\ b} = \iint_{t\ or\ b} q_{(x,y)}^* \times \cos\left(\delta\kappa_y y^*\right) dy^* dx^* \tag{17}$$

$$s_{mn}^{t\ or\ b} = \iint_{t\ or\ b} q_{(x,y)}^* \times \cos\left(\lambda\kappa_x x^*\right)\cos\left(\delta\kappa_y y^*\right) dx^* dy^* \tag{18}$$

From Eq. (8) one can see that the conservation of energy in the plate is automatically satisfied.

*ii) Multiple sources/sinks on the top and bottom surface*

Since conduction heat transfer in a solid is a linear process, superposition principle is applicable. As such, for cases with

multiple sources/sinks on each of the top and bottom surfaces, temperature distribution can be readily obtained by superposing the single source results. Using this approach, the solution can be generalized for rectangular plates with 'M' and 'N' number of sources/sinks on the top and bottom surfaces, respectively. As a result, the solution, Eq. (6), and the coefficients, Eqs. (8-14), remain unchanged, however; the auxiliary coefficients take the more general form of below:

$$s_{00}^{t\ or\ b} = \iint_{t\ or\ b} q_{i(x,y)}^{*}\, dx^{*} dy^{*} \tag{19}$$

$$s_{m0}^{t\ or\ b} = \iint_{t\ or\ b} q_{i(x,y)}^{*} \times \cos\left(\lambda\kappa_x x^{*}\right) dx^{*} dy^{*} \tag{20}$$

$$s_{0n}^{t\ or\ b} = \iint_{t\ or\ b} q_{i(x,y)}^{*} \times \cos\left(\delta\kappa_y y^{*}\right) dy^{*} dx^{*} \tag{21}$$

$$s_{mn}^{t\ or\ b} = \iint_{t\ or\ b} q_{i(x,y)}^{*} \times \cos\left(\lambda\kappa_x x^{*}\right)\cos\left(\delta\kappa_y y^{*}\right) dx^{*} dy^{*} \tag{22}$$

Using the above auxiliary coefficients, the temperature distribution inside an anisotropic plate can be found for any number and arrangement of heat sources and sinks.

**Special case:** in a particular case, in which each spot has a constant heat flux $q_i$, the general auxiliary coefficients take the following simplified form:

$$s_{00}^{t\ or\ b} = \sum_{i=1}^{M\ or\ N} q_i^{*} a_i^{*} b_i^{*} \tag{23}$$

$$s_{m0}^{t\ or\ b} = \frac{1}{\lambda\kappa_x} \sum_{i=1}^{M\ or\ N} q_i^{*} b_i^{*} \sin(\lambda\kappa_x x^{*})\Big|_{X_i^{*}-\frac{a_i^{*}}{2}}^{X_i^{*}+\frac{a_i^{*}}{2}} \tag{24}$$

$$s_{0n}^{t\ or\ b} = \frac{1}{\delta\kappa_y} \sum_{i=1}^{M\ or\ N} q_i^{*} a_i^{*} \sin(\delta\kappa_y y^{*})\Big|_{Y_i^{*}-\frac{b_i^{*}}{2}}^{Y_i^{*}+\frac{b_i^{*}}{2}} \tag{25}$$

$$s_{mn}^{t\ or\ b} = \frac{1}{\lambda\delta\kappa_x\kappa_y} \sum_{i=1}^{M\ or\ N} q_i^{*} \sin(\lambda\kappa_x x^{*})\Big|_{X_i^{*}-\frac{a_i^{*}}{2}}^{X_i^{*}+\frac{a_i^{*}}{2}} \times \sin(\delta\kappa_y y^{*})\Big|_{Y_i^{*}-\frac{b_i^{*}}{2}}^{Y_i^{*}+\frac{b_i^{*}}{2}} \tag{26}$$

### Thermal resistance

To define thermal resistance two temperatures and the amount of heat flow is required [13–16]. In this study, the difference between average temperatures over the heat sources and heat sinks is considered as the temperature difference required for defining the thermal resistance. Total heat flow also can be derived by integrating the heat flux over the heat sources or heat sinks domain. As such, the spreading resistance can be defined as:

$$R^{*} = \frac{\left|\bar{\theta}_{Sources} - \bar{\theta}_{Sinks}\right|}{Q^{*}} \tag{27}$$

where,

$$\bar{\theta}_{Sources} = \frac{1}{\sum_{Sources} a_i^{*} b_i^{*}} \sum_{Sources} \int_{Y_i^{*}-\frac{b_i^{*}}{2}}^{Y_i^{*}+\frac{b_i^{*}}{2}} \int_{X_i^{*}-\frac{a_i^{*}}{2}}^{X_i^{*}+\frac{a_i^{*}}{2}} \theta_{Sources}\, dx^{*} dy^{*} \tag{28}$$

$$\bar{\theta}_{Sink} = \frac{1}{\sum_{Sinks} a_i^{*} b_i^{*}} \sum_{Sinks} \int_{Y_i^{*}-\frac{b_i^{*}}{2}}^{Y_i^{*}+\frac{b_i^{*}}{2}} \int_{X_i^{*}-\frac{a_i^{*}}{2}}^{X_i^{*}+\frac{a_i^{*}}{2}} \theta_{Sink}\, dx^{*} dy^{*} \tag{29}$$

$$Q^{*} = \left| \iint_{Sources/Sinks} q_i^{*} dx^{*} dy^{*} \right| \tag{30}$$

For the case of constant heat fluxes, $Q^{*}$ can simply be calculated by summation of dimensionless heat fluxes multiplied by their dimensionless domain area.

## RESULTS AND DISSCUSION

### Model validation

To validate the present model, an anisotropic rectangular Pyrolytic Graphite Sheet (PGS) with an arbitrary arrangement of four spots, i.e., two sources on the top surface and two sinks on the bottom is assumed, see Fig. 3. The chosen PGS has through-plane thermal conductivity of 4W/m.K and in-plane one of 800W/m.K [4–6].

The numerical analysis is performed using COMSOL Multiphysics 4.2a [19]. A sensitivity study on the grid size is performed for two different levels of extra and extremely fine mesh sizes with 7.6×104 and 4.2×105 elements, respectively. Less than 0.1 percent relative difference for local temperature between the two cases is observed. The computation time for the extra fine mesh size using a typical Pentium Dual-Core PC is around 20 seconds.

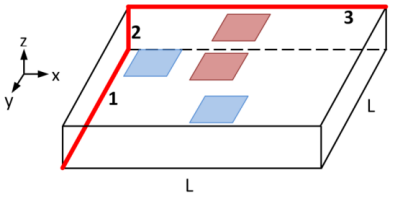


**Figure 1.** Cut-lines' position inside the rectangular plate for comparison between the analytical and numerical results

To compare the results quantitatively, temperatures along three different imaginary lines in three different directions, labeled in Fig. 3, are plotted in Fig. 4 for both analytical and numerical results. For this specific example, the characteristic length, L, and are equal to 0.1m and 1kW, respectively. Thermal conductivity in z-direction is assumed to be 4W/m.K. The thermo-physical parameters are listed in Table 1.

Table 1. Thermo-physical characteristics of the plate and the spots in Fig. 3 used in the numerical analysis.

| Plate dimensions | Plate material | Source 1 | Source 2 | Sink 1 | Sink 2 |
|---|---|---|---|---|---|
| L=1cm | $k_z$=4W/mk | | $Q_{ref}$ =1kW | | |
| ε=1 | $\kappa_x$=0.25 | $a^*$=0.2 | $a^*$=0.2 | $a^*$=0.2 | $a^*$=0.2 |
| $\varepsilon_H$=0.2 | $\kappa_y$=0.50 | $b^*$=0.2 | $b^*$=0.2 | $b^*$=0.2 | $b^*$=0.2 |
| | | $X^*$=0.5 | $X^*$=0.5 | $X^*$=0.5 | $X^*$=0.2 |
| | | $Y^*$=0.5 | $Y^*$=0.8 | $Y^*$=0.5 | $Y^*$=0.9 |
| | | $q^*$=1 | $q^*$=1 | $q^*$=1 | $q^*$=1 |

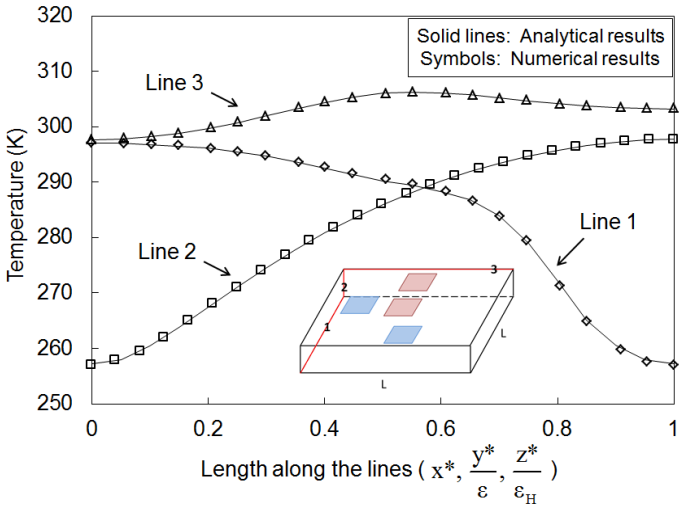


**Figure 2.** Comparison between the present analytical model and numerical results for temperature along three different cut-lines. The hotspots arrangement of Fig. 3 was used.

As shown in Fig. 4, there is an excellent agreement between the analytical model results and the numerical simulation. A sensitivity analysis on the number of eigenvalue terms in the series solution is performed. Increasing the number of terms in the series from 100 to 400 will not change the solution considerably (less than 0.1%).

**Parametric study**

A parametric study is performed to investigate the effects of anisotropy on thermal performance of heat spreaders. This parametric study is conducted for spreaders with single heat source and heat sink, each of them placed on one face of the plate. The behavior of the multi-hotspot geometries can be obtained by superposing the effects caused by each single spot.

To cover a wide range of source/sink relative position and see the effect of anisotropy, two different arrangements for source and sink are chosen to represent two extreme cases, as shown in Fig. 5. In the first case, a heat source on the top and a heat sink on the bottom are centrally aligned and positioned at the center of the plate. This arrangement (Case I) represents the lowest thermal resistance due to the minimum distance between the source and the sink. In Case II, the heat source on the top surface and the heat sink on the bottom surface are positioned at two opposite corners; thus representing the highest thermal resistance. Heat sources and heat sinks are assumed to be isoflux.

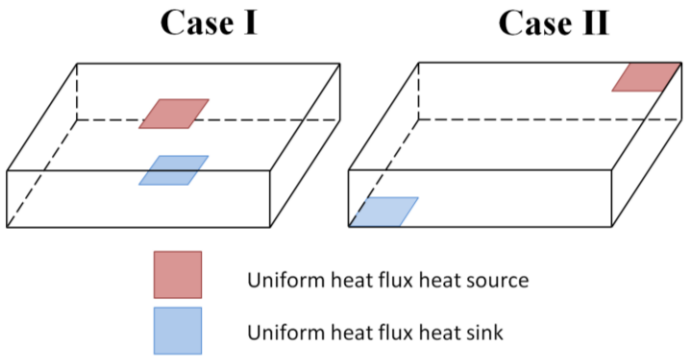


**Figure 3.** Two different arrangements of hotspots for parametric study (left: Case I, Right: Case II).

To study the anisotropy of materials, resistance of square plate with two different arrangements of source and sink, Case I and Case II, Fig. 5, is plotted versus through-plane to in-plane conductivity ratios for four different plate thicknesses in Figs. 6 and 8. Conductivity ratio ($k_{xy}/k_z$) ranges from 0.01 to 100. The source and sink are identical squares with arbitrary side length of 0.2L. The plate is also set to be square ($\varepsilon=W/L=1$). The effect of spots size will be investigated separately later. For better depiction, the graphs are plotted in logarithmic scale.

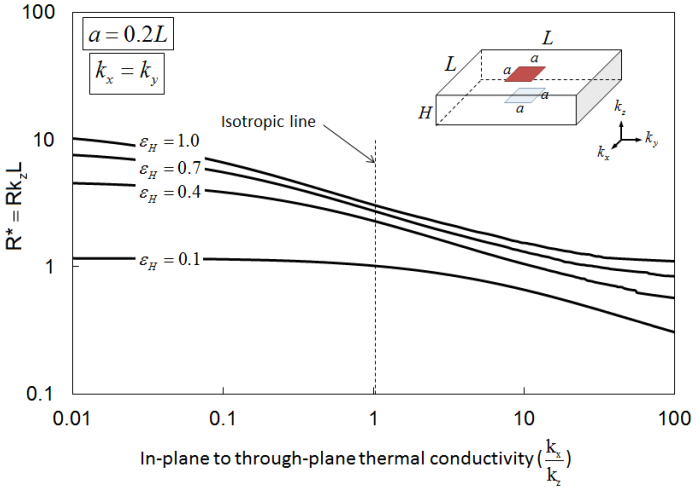


**Figure 4.** Resistance versus through-plane to in-plane conductivity ratio for four thicknesses (Case I)

Figure 6 shows, in a plate with two centrally-aligned spots on the top and bottom (Case I), as the ratio of the in-plane to through-plane conductivity increases, the thermal resistance decreases. This trend can be explained as follows: as the in-plane conductivity increases, the temperature becomes uniform over the surface much faster due to less in-plane resistance against the heat flow, so the heat spreading/constriction takes place easier with less temperature drop.

For the arrangement of Case I, heat transfer improvement due to increasing the in-plane conductivity is directly related to the size of the spots. As shown in Fig. 7, for smaller spot area,

the resistance decrease occurs more significantly when the in-plane thermal conductivity increases. This is due to the fact that the spreading/constriction resistance becomes more considerable with smaller relative spot sizes. Thus, in such spreaders, higher in-plane thermal conductivity results in much better thermal performance improvement of the heat spreader. In other words, for smaller spots it is thermally more efficient to use anisotropic material for spreader. At the limit where the spot's sizes are as big as the plate surface, i.e., 1-D heat conduction, no spreading or constriction exists thus changing the in-plane conductivity has no effect on the plate resistance.

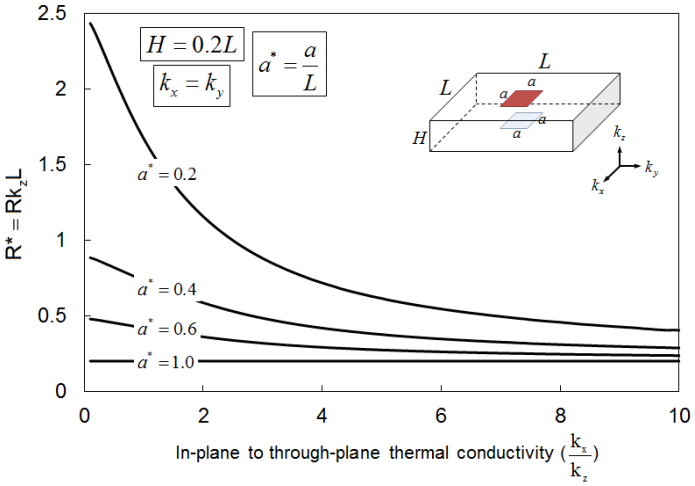


**Figure 5.** Resistance versus through-plane to in-plane conductivity ratio for four hotspot size (Case I)

For the second arrangement (Case II), anisotropy of the material has a more pronounced effect on the thermal performance of the spreader. Figure 8 presents the resistance variation of the plate as the in-plane to through-plane conductivity ratio changes from 0.01 to 100. It shows, for all the thicknesses, thermal resistance decreases as the in-plane conductivity increases. For thinner plates, this variation is more than thicker ones. For thin plates the heat coming from the heat source at one corner has to pass through the smaller cross-section than the thicker plates to reach the heat sink at the other corner, resulting in higher resistance for thinner plates. But as the in-plane thermal conductivity increases, the effect of in-plane resistance becomes less important and the thickness becomes the controlling parameter. This phenomenon is clearly shown in Fig. 8, where two curves of different thicknesses intersect. These intersection points demarcate the critical conductivity ratios for the two corresponding thicknesses before which the in-plane resistance is dominant, thus thinner plate has larger resistance. However, beyond these points, through-plane heat transfer plays a more important role, and the thicker plate presents more resistance.

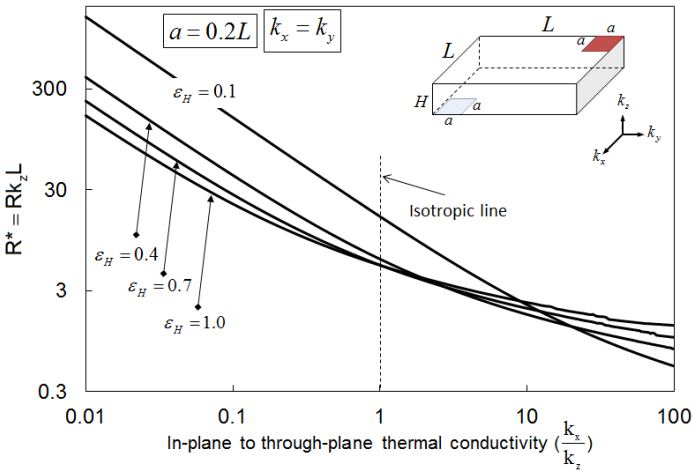


**Figure 6.** Resistance versus through-plane to in-plane conductivity ratio for four thicknesses (Case II)

The important points can be summarized as,

- Regardless of spots arrangement and plate thickness, increasing the in-plane thermal conductivity always improve the heat transfer.
- As the relative eccentricity of spots on the top and bottom surface increases, the anisotropy effect becomes more prominent.
- As the relative size of spots becomes smaller, increasing in-plane thermal conductivity has a more pronounced effect on the thermal performance of the plate.
- Changing anisotropy in thinner plates creates more resistance variation compared to thicker ones.
- In 1-D heat transfer, resistance is only a function of through-plane conductivity and the plate material's anisotropy has no effect on its resistance.

## SUMMARY

A new analytical model was developed for temperature distribution inside anisotropic rectangular plates subjected to multiple cold/hotspots on the top and bottom surfaces. 2-D Fourier expansion technique was used to transform the discrete Neumann boundary conditions on the top and bottom into a continuous form. The solution was first developed for the case with arbitrary single spot on each side and then using the superposition principle, it was extended to the general form to cover multi-spot cases. The model was validated by an independent numerical simulation data and a perfect agreement was observed. Thermal spreading resistance then was defined for the plate and a parametric study for optimization purpose was performed. The effects of anisotropy on the resistance were discussed in detail.

## REFERENCES


[1] W. Kuo, T. Wu, H. Lu, and T. Lo, "Microstructures and Mechanical Properties of Nano-Flake Graphite Composites," in *16th International Conference on Composite Materials*, 2007.

[2] L. Dai, "Functionalization of Graphene for Efficient Energy Conversion and Storage," *Accounts of chemical research*, vol. 46, no. 1, pp. 31–42, 2013.

[3] D. D. L. Chung and Y. Takizawa, "Performance of Isotropic and Anisotropic Heat Spreaders," *Journal of Electronic Materials*, vol. 41, no. 9, pp. 2580–2587, Jun. 2012.

[4] J. Norley, J. Tzeng, and G. Getz, "The Development of a Natural Graphite Heat-Spreader," in *Seventeenth IEEE SEMI*, 2001, pp. 107–110.

[5] Y. Taira, S. Kohara, and K. Sueoka, "Performance improvement of stacked graphite sheets for cooling applications," *2008 58th Electronic Components and Technology Conference*, pp. 760–764, May 2008.

[6] Panasonic Electronic Devices Co., "Pyrolitic Graphite Sheet." [Online]. Available: http://www.panasonic.com/industrial/demo/en_demo.asp.

[7] K. F. Kelly and W. E. Billups, "Synthesis of soluble graphite and graphene.," *Accounts of chemical research*, vol. 46, no. 1, pp. 4–13, Jan. 2013.

[8] M. M. Yovanovich, Y. S. Muzychka, and J. R. Culham, "Spreading Resistance of Isoflux Rectangles and Strips on Compound Flux Channel," *Journal of Thermophysics and Heat Transfer*, vol. 13, no. 4, pp. 495–500, 1999.

[9] S. Karmalkar, P. V. Mohan, and B. P. Kumar, "A unified compact model of electrical and thermal 3-D spreading resistance between eccentric rectangular and circular contacts," *IEEE Electron Device Letters*, vol. 26, no. 12, pp. 909–912, Dec. 2005.

[10] A. G. Kokkas, "Thermal Analysis of Multiple-Layer Structures," *IEEE Transaction on Electron Devices*, vol. ED-21, no. 11, pp. 674–681, 1974.

[11] V. Kadambi and N. Abuaf, "An Analysis of the Thermal Response of Power Chip Packages," *IEEE Transaction on Electron Devices*, vol. ED-32, no. 6, pp. 1024–1033, 1985.

[12] J. R. Culham, M. M. Yovanovich, and T. F. Lemczyk, "Thermal Characterization of Electronic Packages Using a Three-Dimensional Fourier Series Solution," *Journal of Electronic Packaging*, vol. 122, no. 3, p. 233, 2000.

[13] Y. S. Muzychka, J. R. Culham, and M. M. Yovanovich, "Thermal Spreading Resistances In Rectangular Flux Channels Part II - Edge Cooling," in *36th AIAA Thermophysics Conference*, 2003.

[14] Y. S. Muzychka, J. R. Culham, and M. M. Yovanovich, "Thermal Spreading Resistance of Eccentric Heat Sources on Rectangular Flux Channels," *Journal of Electronic Packaging*, vol. 125, no. 2, pp. 178–185, 2003.

[15] Y. S. Muzychka, "Influence Coefficient Method for Calculating Discrete Heat Source Temperature on Finite Convectively Cooled Substrates," *IEEE Transactions on Components and Packaging Technologies*, vol. 29, no. 3, pp. 636–643, Sep. 2006.

[16] B. Dan, J. F. Geer, and B. G. Sammakia, "Heat Conduction in a Rectangular Tube With Eccentric Hot Spots," *Journal of Thermal Science and Engineering Applications*, vol. 3, no. 4, p. 041002, 2011.

[17] T. M. Ying and K. C. Toh, "A heat spreading resistance model for anisotropic thermal conductivity materials in electronic packaging," in *The Seventh Intersociety Conference on Thermal and Thermomechanical Phenomena in Electronic Systems (Cat. No.00CH37069)*, 2000, pp. 314–321.

[18] Y. S. Muzychka, M. M. Yovanovich, and J. R. Culham, "Thermal Spreading Resistance in Compound and Orthotropic Systems," *Journal of Thermophysics and Heat Transfer*, vol. 18, no. 1, pp. 45–51, Jan. 2004.